Estimation of Purkinje Activation from ECG: an Intermittent Left Bundle Branch Block Study

Sophie Giffard-Roisin, Lauren Fovargue, Jessica Webb, Roch Molléro, Jack Lee, Hervé Delingette, Nicholas Ayache, Reza Razavi, Maxime Sermesant

Estimation of Purkinje Activation from ECG: an Intermittent Left Bundle Branch Block Study

Sophie Giffard-Roisin[1], Lauren Fovargue[2], Jessica Webb[2], Roch Molléro[1], Jack Lee[2], Hervé Delingette[1], Nicholas Ayache[1], Reza Razavi[2], and Maxime Sermesant[1]

[1] Inria, Asclepios Research Project, France.
[2] Department of Biomedical Engineering, King's College London, United Kingdom.

Abstract. Modelling the cardiac electrophysiology (EP) can help understand pathologies and predict the response to therapies such as cardiac resynchronization. To this end, estimating patient-specific model parameters is crucial. In the case of patients with bundle branch blocks (BBB), part of the Purkinje system is often affected. The aim of this work is to estimate the activation of the right and left Purkinje systems from standard non-invasive techniques: magnetic resonance imaging (MRI) and 12-lead electrocardiogram (ECG). As it is difficult to differentiate the contribution of the Purkinje system, this work relies on a particular intermittent left BBB (LBBB) case where both LBBB and absence of LBBB (ALBBB) were recorded on different 12-lead ECGs. First, an efficient forward EP model is proposed by coupling a Mitchell-Schaeffer cardiac model with a current dipole formulation that simulates the ECG. We used the Covariance Matrix Adaptation Evolution Strategy (CMA-ES) algorithm to optimize the 3 parameters by minimizing the error with the real ECG. The estimation of conduction velocity (CV) parameters for LBBB and ALBBB shows a good agreement on the myocardial CV ($0.39m/s$ for ABBB, $0.40m/s$ for LBBB), while the estimation of the left Purkinje CV seems to identify the pathology ($1.32m/s$ for ALBBB, $0.49m/s$ for LBBB). Finally, the plots of the simulated 12-lead ECGs together with the ground truth ECGs indicate similar shapes.

Keywords: Electrophysiology, Electrophysiological Model, Forward EP Model, Parameter Estimation, Purkinje System

1 Introduction

Modelling the cardiac electrophysiology (EP) can help understanding pathologies and predicting the response to therapies such as cardiac resynchronization therapies (CRT). To this end, estimating patient-specific model parameters is crucial. In the case of patients with bundle branch blocks (BBB), part of the Purkinje system is often affected. The Purkinje fibers are located just beneath the endocardium and are able to conduct cardiac action potentials quickly and efficiently: typical conduction velocity (CV) ranges from 2 to $3m/s$ while it ranges from 0.3 to $0.4m/s$ for myocardial cells [1]. Stimulus arrives from the

atrioventricular node through the His bundle and separate the network in two branches, the left bundle and the right bundle. When a block occurs in a bundle (LBBB for left, RBBB for right), the Purkinje system is not as efficient and the contraction of the ventricles isn't synchronized.

Some studies have been focusing on the understanding of LBBB patterns by simulating ECGs with different parameters from precise cardiac and torso models [2, 3]. Because of their complexity, we defined a simpler model for the estimation of patient-specific parameters. A study has also recently proposed an EP parameter estimation from ECG data [4]. It uses two features from the 12-lead ECG to recover 3 electrical diffusivity parameters using a boundary element method forward model and a polynomial regression. As it is difficult to differentiate the contribution of the Purkinje system, our work relies on a particular intermittent LBBB case where both LBBB and absence of LBBB (ALBBB) are recorded on 12-lead ECGs. First, an efficient forward EP model is proposed by coupling a 3-parameter cardiac EP model based on the Mitchell-Schaeffer model with a current dipole formulation. We used the CMA-ES algorithm to optimize the 3 parameters by minimizing the error with the ECG signals.

2 Materials and Methods

2.1 Clinical Data

In this study, we considered cardiac imaging data from MRI and electrical data from the 12-lead ECG. The MRI acquisition allows a precise myocardial geometry at end diastole. The 12-lead ECG represents the cardiac electrical activity recorded from 9 body surface electrodes. Because the locations of the electrodes were not registered, we manually position them guided by the conventional ECG placement (Figure 1(a)). The 12 standard Einthoven, Goldberger and Wilson leads (12-lead ECG) measures the potential differences between selected electrodes.

2.2 Pre-processing

The myocardial mesh was generated using the VP2HF platform [6] and the VP2HF meshing pipeline[1] creating a tetrahedral mesh with roughly 90K tetrahedra. Rule-based fibre directions were estimated with an elevation angle between $-70°$ and $70°$. The right and left Purkinje regions were manually delineated (Figure 1(b)). The 12-lead ECG were digitized using the opensource Engauge Digitizer followed by a resampling at a rate of 1kHz. Only the 200ms following the Q wave were used (QRS window).

[1] VP2HF is a European Seventh Framework Program, http://www.vp2hf.eu/. The VP2HF meshing pipeline is based on CGAL, VTK, ITK and VMTK opensources libraries.

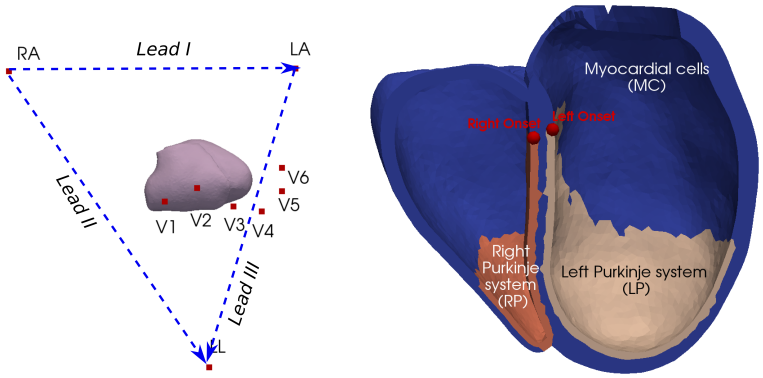

(a) (b)

Fig. 1. (a) The 9 ECG electrodes and the cardiac mesh. (b) Long axis view of the cardiac mesh with delineated regions: Myocardial cells region (blue), right Purkinje system region (orange) and left Purkinje system region (beige). The red dots are the modeled right and left onset activation locations.

2.3 Forward EP Model

Mitchell-Schaeffer Cardiac Model: We simulated the electrical activation of the heart using the monodomain version of the Mitchell-Schaeffer's EP model [7]. The monodomain formulation considers that the extra-cellular and intra-cellular anisotropies are proportional and therefore we can solve directly the transmembrane potential. It is governed by:

$$C_m \frac{\partial v}{\partial t} + I_{ion} = \nabla \cdot \boldsymbol{\sigma} \nabla v \tag{1}$$

with v the transmembrane potential, C_m the membrane capacitance and I_{ion} the current through the cell membrane per unit of area. The anisotropic conduction tensor $\boldsymbol{\sigma}$ is defined as $\boldsymbol{\sigma} = \sigma \cdot diag(1, r, r)$ where the anisotropy ratio r enables conduction velocity in the fibre direction to be larger than in the transverse plane (we used $r = (1/2.5)^2$). The conductivity σ is a local parameter that depends on the capability of the tissue to propagate the electrical activation. σ can be written in terms of intracellular and extracellular conductivities: $\sigma = \frac{\sigma^i \sigma^e}{\sigma^i + \sigma^e}$ The reduction of the monodomain model implies $\sigma^i = \lambda \sigma^e$ for some scalar λ resulting in a linear relationship between σ and σ^i. The diffusivity d (in $m^2 s^{-1}$) can be expressed as a conductivity σ (in $\Omega.m$) by using $\sigma = C_m \beta\, d$ with C_m the membrane capacitance and β the surface-to-volume ratio. Finally, the diffusion d is linked to the conduction velocity c in m/s by $c = k\sqrt{d}$, where the constant k was estimated numerically in our simulations as $0.35\, s^{-1/2}$.

In this work, we considered 3 different domains with uniform conduction velocities: the myocardial cells (MC), the left Purkinje system (LP) and the

right Purkinje system (RP). The MC was modelled as one single domain for simplification reasons and because the patient was non-ischaemic. We modelled the LP and RP as a thin layer covering the endocardial surfaces. By considering that the Purkinje geometry is unknown, this simplification to a layer allows also a rapid computation. Concretely, the layer is composed of all the tetrhedra connected to the endocardial surface.

We manually selected the onset activation locations on the septum near the valves, see Figure 1(b). This was driven by the fact that the electrical wave arrives from the His bundle to the left and right bundles located on the septum.

From Cardiac Simulations to BSPM, Current Dipole Formulation: We computed simultaneously the cardiac electrical sources and body surface potentials. Our forward method is based on a simplified framework composed of sources and sensors in an infinite and homogeneous domain. As in [5], we modelled every myocardium volume element (tetrahedron) as a spatially fixed but time varying current dipole. The equivalent current density $\mathbf{j}_{eq}$ writes as:

$$\mathbf{j}_{eq} = -\sigma^i \nabla v \tag{2}$$

$\mathbf{j}_{eq}$ is a current dipole moment per unit of volume and the local dipole moment $\mathbf{p}$ in the volume V writes as $\mathbf{p} = \int_V \mathbf{j}_{eq} dV$.

According to the volume conductor theory, the electric potential at a distance R in a homogeneous volume conductor of conductivity σ_T is:

$$\Psi(R) = \frac{1}{4\pi\sigma_T} \int_V \mathbf{j}_{eq} \cdot \nabla(\frac{1}{R}) dV \tag{3}$$

The infinitesimal dipole moment of the volume dV_X located at position X is defined as $\mathbf{p}_X = \mathbf{j}_{eq,X}\, dV_X = -\sigma^i_X\, \nabla v_X dV_X$. As we use linear tetrahedra in the FEM discretization of the myocardium, the potential v is linear and ∇v is constant over the tetrahedron. We get the following formulation of the dipole moment of the charge in the volume V_H of tetrahedron H of the myocardial mesh: $\mathbf{p}_H = -\sigma^i_H \nabla v_H V_H$.

From [8], the gradient of the electric potential in tetrahedron H can be computed from the potentials $v(X^k_H)$ at the nodes X^k_H, and the contribution Ψ_H of the tetrahedron H to the potential field calculated at position X_T is:

$$\Psi_H(X_T) = \frac{1}{4\pi\sigma_T} \frac{\sigma^i_H V_H\, (\nabla v_H \cdot \overrightarrow{HT})}{\|\overrightarrow{HT}\|^3} \tag{4}$$

with $\overrightarrow{HT}$ the vector from centre of the tetrahedron H to the torso electrode location T. Finally, we sum over the whole mesh to get the potential field at X_T. The implementation was performed using the SOFA platform[2], with a direct coupling to the Mitchell-Schaeffer model. One iteration of the model is computed in 0.1ms (dual-Xeon X6570 with 12 cores at 2.93GHz).

[2] SOFA is an Open Source medical simulation software available at http://www.sofa-framework.org

2.4 Parameter Estimation using CMA-ES Algorithm

We estimated the 3 conduction parameters using a Covariance Matrix Adaptation Evolution Strategy (CMA-ES) [9]. It is a derivative-free and stochastic algorithm that is suited for non-convex continuous optimization problems. At each iteration, new candidate solutions are sampled from a multivariate normal distribution whose covariance matrix is adapted according to the ranking between the candidate solutions of the previous iteration. We define the score of a simulation S as its error to the ground truth 12-lead ECGs Ψ_{GT}:

$$f(S) = \int_{t=0}^{T} \frac{1}{N} \sum_{i=1}^{N} |\Psi_{GT}(i,t) - \frac{\|\Psi_{GT}\|}{\|\Psi_S\|}\Psi_S(i,t)| \tag{5}$$

with N the number of leads ($N = 12$), T the final time ($T = 200ms$), $\Psi_{GT}(i,t)$ the ground truth difference of potential of the lead i at time t and $\Psi_S(i,t)$ the simulated difference of potential of the lead i at time t. We used a population of 100 simulations per generation and optimized over 20 generations. We initialized the algorithm by a multivariate distribution of mean $x_0 = (0.6, 0.6, 0.6)m/s$ and standard deviation $std = 0.1m/s$ in each direction. We fix the parameter searching range at $[0.05, 2.5]m/s$ to avoid non-physical solutions. The best score vs, the number of iterations for a parameter estimation is plotted on Figure 2.4.

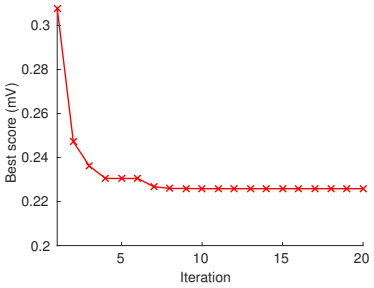

Fig. 2. Best score versus the number of iterations of the CMA-ES algorithm. The score is identified as the mean error between the simulated and real 12-lead ECG, in mV.

3 Evaluation on an Intermittent LBBB Patient

3.1 Intermittent LBBB Patient Data

As an evaluation of the proposed method, a patient with intermittent LBBB was chosen. The data has been acquired at St Thomas Hospital (London) as part of the VP2HF project. Both LBBB pattern and absence of LBBB (ALBBB) were documented on two 12-lead ECG, the ALBBB being recorded after the LBBB.

The parameters were estimated separately for the LBBB and ALBBB. Only the right onset location was activated for the LBBB whereas both right and left were activated for ALBBBm because in an LBBB the left bundle is not active.

3.2 Results

Table 1 shows the CV before the parameter estimation, after the LBBB parameter estimation and after the ALBBB parameter estimation. First, all Purkinje CV are higher than myocardial CV which is to be expected. We can see that the myocardial cells CV (as for the right Purkinje) is very similar between the LBBB and the ALBBB estimations. For the left Purkinje, we found $0.49m/s$ for LBBB and $1.32m/s$ for ALBBB, indicating that the model seems to identify the LBBB pathology (affected LP system). Moreover, the MC CV values lie in the myocardial CV range found in the literature [1]. The RP CV (as well as the LP CV for the ALBBB) is close to the Purkinje CV range found in the literature.

Table 1. Estimated Conduction Velocities for LBBB and ALBBB.

$CV(m/s)$	**myocardium**	**left Purkinje**	**right Purkinje**
Initially	0.6	0.6	0.6
LBBB	0.39	0.49	0.95
Absence of LBBB	0.40	1.32	1.22

Figure 3 shows the simulation results after parameter estimation. Figure 3(a) represents the true (black) and simulated (blue) 12-lead ECG for the LBBB case and Figure 3(b) the corresponding cardiac activation map. We can see that the shape of the ECG is coherent with the ground truth and especially the clear notched R wave on leads V5 and V6, indicator of an LBBB pathology. Figures 3(c) and 3(d) depict the results for the ALBBB, where both QRS on ECG and activation times are shorter than for the LBBB. The real and simulated ECG for ALBBB have similar shapes even though we can notice the notched V2 and V3 R waves (so RV and LV are not perfectly synchronous). It may indicate that our Purkinje zone delimitation could be improved.

4 Discussion

We have shown a promising parameter estimation based on common non-invasive procedures and identified the activation of the Purkinje system. The fact that the RP and LP conductions are smaller than the literature range could be due to the fact that we model the Purkinje system as a layer (and not a small fiber network). For consitency reasons, we initialized the LBBB with only the right onset. However, it leads to different initial settings between ALBBB and LBBB parameter estimation. That is why we also ran our algorithm using both onsets

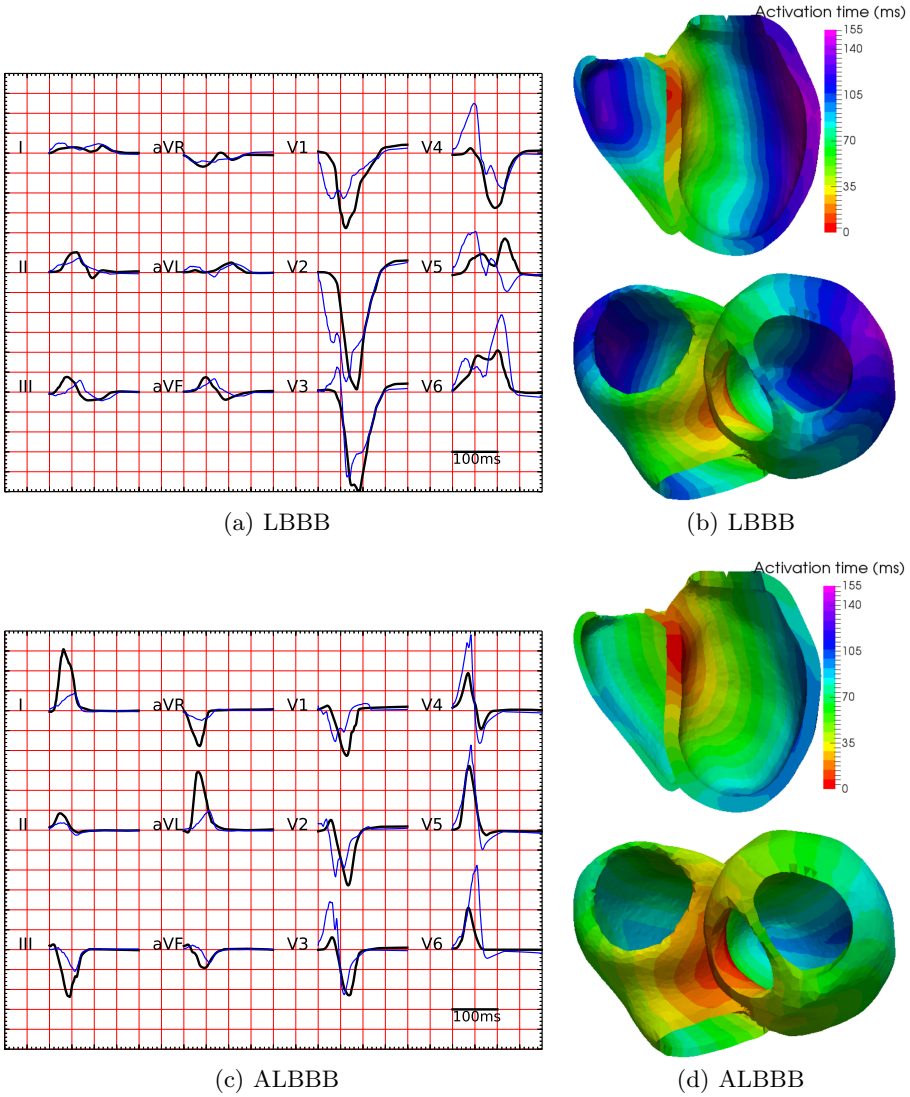

(a) LBBB (b) LBBB

(c) ALBBB (d) ALBBB

Fig. 3. Simulation results after parameter estimation. *LBBB:* (a) Real 12-lead ECG (black) and estimated (blue) during the 200 ms after onset activation. (b) Estimated activation map. *ALBBB:* (c) Real 12-lead ECG (black) and estimated (blue) during the 200 ms after onset activation. (d) Estimated activation map.

for the LBBB: we found a similar left Purkinje CV. Because of the simplicity of the 12-lead ECG, we made some strong assumptions as the location of the onset activation and of the torso electrodes. This could lead to important errors and may not allow to identify more model parameters. We can think of two ways to avoid this problem. The first consists in using BSPM data with more electrodes and recorded locations. The second includes the processing of more patient data to identify the error distribution.

5 Conclusion

We have shown a method for estimating the activation of the left and right Purkinje system of the EP cardiac model based on the 12-lead ECG. The estimation of CV parameters for LBBB and ALBBB (same patient) shows a good agreement for the myocardium CV ($0.39m/s$ for ABBB, $0.40m/s$ for LBBB), while the estimation of the left Purkinje CV seems to identify the pathology ($1.32m/s$ for ALBBB, $0.49m/s$ for LBBB). Moreover, the plots of the simulated 12-lead ECGs and the real ECGs indicate similar shapes. We believe this work to be an interesting first step for understanding and modelling BBB pathology.

Acknowledgments. The research leading to these results has received funding from the Seventh Framework Programme (FP7/2007-2013) under grant agreement VP2HF n°611823.

References

1. Durrer, Dirk et al.: Total excitation of the isolated human heart. In: Circulation, pp. 899–912, vol. 41. Am Heart Assoc (1970)
2. Lorange, M. et al.: A computer heart model incorporating anisotropic propagation. In: Journal of Electrocardiology, pp. 263–277, vol. 26. Elsevier (1993)
3. Potse, M. et al.: Similarities and differences between electrocardiogram signs of left bundle-branch block and left-ventricular uncoupling. In: Europace, pp. v33–v39, vol. 14. Eur Heart Rhythm Assoc (2012)
4. Zettinig, O. et al.: Data-driven estimation of cardiac electrical diffusivity from 12-lead ECG signals. In: Medical image analysis, pp. 1361–1376, vol. 18. Elsevier (2014)
5. Chávez, C. et al.: Inverse problem of electrocardiography: Estimating the location of cardiac ischemia in a 3d realistic geometry. In: International Conference on Functional Imaging and Modeling of the Heart, pp. 393–401. Springer (2002)
6. Groth, A and Weese, J and Lehmann, H: Robust left ventricular myocardium segmentation for multi-protocol MR. In: SPIE Medical Imaging, pp. 83142S–83142S. International Society for Optics and Photonics (2012)
7. Mitchell, C. and Schaeffer, D.: A two-current model for the dynamics of cardiac membrane. In: Bulletin of mathematical biology, pp. 767–793, vol. 65. Springer Berlin Heidelberg (2003)
8. Delingette, Hervé and Ayache, Nicholas: Soft tissue modeling for surgery simulation. In: Handbook of Numerical Analysis, pp. 453–550, vol. 12. Elsevier (2004)
9. Hansen, N.: The CMA evolution strategy: a comparing review. In: Towards a new evolutionary computation, pp. 75–102. Springer Berlin Heidelberg (2006)